Analytical results for Josephson dynamics of ultracold bosons

Lena Simon and Walter T. Strunz
Institut für Theoretische Physik, Technische Universität Dresden, D-01062 Dresden, Germany
(Received 5 October 2012; published 26 November 2012)

We study the dynamics of ultracold bosons in a double-well potential within the two-mode Bose-Hubbard model by means of semiclassical methods. By applying a Wentzel-Kramers-Brillouin (WKB) quantization we find analytical results for the energy spectrum, which are in excellent agreement with numerically exact results. They are valid in the energy range of plasma oscillations, both in the Rabi and the Josephson regime. Adopting the reflection principle and the Poisson summation formula we derive an analytical expression for the dynamics of the population imbalance depending only on the few relevant parameters of the system. This allows us to discuss its characteristic dynamics, especially the oscillation frequency and the collapse and revival time, as a function of the model parameters, leading to a deeper understanding of Josephson physics. We find that our formulas match previous experimental observations.

DOI: 10.1103/PhysRevA.86.053625 PACS number(s): 03.75.Lm, 03.65.Sq, 05.30.−d

I. INTRODUCTION

Fundamental issues of nonequilibrium physics of interacting many-body quantum systems and of phase coherence and phase stability, in particular, have a long history. A simple yet relevant model, the two-site Bose-Hubbard Hamiltonian, features phase and fluctuation decay and also revivals and thus, over the years, many thorough investigations of its quantum dynamics have appeared. Most remarkably, recent experiments involving ultracold Bose gases trapped in an effectively one-dimensional double-minimum potential represent an almost ideal realizations of this fundamental model [1,2], with the fascinating possibility to vary relevant model parameters over a wide range.

A full many-body calculation of the dynamics of an interacting, trapped ultracold Bose gas is only possible for a very small number of particles, even for weakly interacting bosons. Most often a mean-field approximation in form of the Gross-Pitaevskii equation is applied, which provides good results for low temperatures and for a large number N of particles, if only for a limited time and for a limited set of observables. These limits are intensively studied. Once the field operators are replaced by a c-number field, some truly quantum phenomena (e.g., wave-function revivals) cannot be described. The double-well potential provides an ideal playground to analyze these issues. Thus, a purely classical-field approach quickly comes to its limits, and the question arises whether *semiclassical* methods can improve the theoretical treatment of such bosonic systems, allowing us in the future to study more challenging problems whose many-body Schrödinger equation can no longer be solved fully numerically.

A number of articles deal with the discussion of the consequences of the mean-field approximation and many-body quantum corrections [3,4] and the many-body quantum and classical dynamics in phase space [5]. Furthermore, semiclassical methods were applied to the double-well system. In Refs. [6–12] a Wentzel-Kramers-Brillouin (WKB) quantization is adopted to analyze the energy spectrum and the wave functions in certain parameter regions.

Despite this fair amount of investigations, it is remarkable to realize that—leaving some fairly straightforward cases aside—no analytical expressions for the relevant dynamical quantities appear to be known. Thus, the purpose of this article is to find a generally applicable analytical description of the population imbalance dynamics of an ultracold Bose gas in a double-well potential by applying semiclassical methods. Since the full quantum dynamics can be determined numerically up to many thousands of particles, we are able to compare with exact results. Clearly, the interesting case of very large $N \to \infty$ can no longer be investigated numerically, yet our analytical approach is suited to study this very limit in detail.

At low temperatures a Bose-Einstein condensate in a double-well potential can be described by a two-mode approximation. The corresponding second-quantized many-particle two-site Bose-Hubbard Hamiltonian is written as

$$\hat{H}_{\mathrm{BH}} = -T(\hat{a}_1^\dagger \hat{a}_2 + \hat{a}_2^\dagger \hat{a}_1) + U(\hat{a}_1^\dagger \hat{a}_1^\dagger \hat{a}_1 \hat{a}_1 + \hat{a}_2^\dagger \hat{a}_2^\dagger \hat{a}_2 \hat{a}_2) + \delta(\hat{n}_1 - \hat{n}_2), \tag{1}$$

with the creation and annihilation operators for a boson in the ith well denoted by $\hat{a}_i^\dagger$, $\hat{a}_i$, respectively, with $[a_i, a_j^\dagger] = \delta_{ij}$. Thus, the particle number operator of the ith site is $\hat{n}_i = \hat{a}_i^\dagger \hat{a}_i$. U is a measure for the on-site two-body interaction strength, T is a tunneling amplitude, which in experiments can be controlled by varying the barrier hight. The tilt parameter δ leads to an asymmetry in the one-particle site energies of the two wells and is used to initiate the dynamics. Note that in the standard notation adapted in Josephson physics we have $E_J = NT$ and $E_C = 4U$ [13].

It has been shown that the Bose-Hubbard Hamiltonian describes the dynamics of the bosons in the double-well potential properly [14], provided that the interaction energy U is small compared to the level spacing of the trap potential, such that only the two lowest-lying modes have to be taken into account. Transverse modes should also be suppressed. It should be mentioned that there are finer descriptions of the two-mode limit that also take into account tunnel coupling energies depending explicitly on the nonlinear two-body interaction

term [15]. In this work, however, we restrict ourselves to the standard Bose-Hubbard Hamiltonian (1).

First, there are three qualitatively quite different regimes [13,16] with respect to crucial features of the energy spectra. They are best explained by introducing the parameter

$$\Lambda = \frac{UN}{T}, \tag{2}$$

which thus separates the Rabi regime ($\Lambda < 1$) from the so-called Josephson regime for which $1 < \Lambda \ll N^2$ and the Fock regime with $\Lambda \gg N^2$.

The Rabi regime is the noninteracting limit $\Lambda \ll 1$, when the system consists of N independent particles leading to an almost harmonic-oscillator energy spectrum and thus, after an initial tilt, to plasma oscillations with the known plasma frequency $\omega_p = 2T\sqrt{1+\Lambda} \approx 2T$ [2,17].

In the Fock regime all eigenenergies are grouped in doublets with a quasidegenerate symmetric and antisymmetric state. Thus, the dynamics of the mean population imbalance follows an extremely slow evolution in time which is called self-trapping.

The Josephson regime combines the two characteristics of the spectrum just discussed. We distinguish the self-trapping regime $E > 2NT$ from the plasma oscillating regime, where $E < 2NT$ holds. In the former regime, the energy eigenstates appear as doublets again leading to self-trapping. In the latter regime, the energy eigenstates correspond to an (anharmonic) oscillator spectrum and the population imbalance oscillates around zero.

Thus, in the Josephson regime the dynamics will depend on the energy of the initial state. For low energies—the subject of this work—the dynamics undergoes plasma oscillations, for higher energies we see self-trapping, which is beyond the scope of this paper.

In this article we have in mind an experiment as in Ref. [1], so the double-well system is initially prepared in the ground state ψ_0 of a tilted potential [i.e., $\delta \neq 0$ in Eq. (1)]. Then, at $t = 0$ it is quickly switched to a symmetric potential (i.e., $\delta = 0$). Starting from an initial population imbalance unequal to zero the system is left to evolve in time.

In our paper we first discuss the spectrum using the semiclassical WKB or Bohr-Sommerfeld quantization. We find a way to systematically obtain an approximate, useful expression for energies in the plasma oscillating regime. In order to describe imbalance dynamics, we need to explore overlap matrix elements in the following section, which we do with the help of the reflection principle. We then apply the Poisson summation formula, which has a long history in semiclassical approaches to quantum dynamics. As a result, we find a useful expression for the time evolution of the imbalance, containing parameters that can be obtained analytically on the basis of the classical Hamiltonian. We then compare exact calculations with our new formula and find remarkable agreement over the whole relevant range of Λ, covering the known Rabi region but also the plasma oscillating Josephson region. In particular, the oscillation frequency and the collapse and revival times are reproduced astonishingly well. We finally discuss the corresponding analytical expressions. It should be noted that the experimentally observed oscillation frequency in Ref. [1] of about 40 ms follows directly from our formula.

II. SEMICLASSICAL DESCRIPTION

We follow mainly Braun [18] and his discrete WKB method, as already applied to the double-well problem by Korsch *et al.* [6]. The two-mode Bose-Hubbard Hamiltonian can be written in the Schwinger spin representation by transforming to angular momentum operators $\hat{J}_x = \frac{1}{2}(\hat{a}_1^\dagger \hat{a}_2 + \hat{a}_2^\dagger \hat{a}_1)$, $\hat{J}_y = \frac{1}{2i}(\hat{a}_1^\dagger \hat{a}_2 - \hat{a}_2^\dagger \hat{a}_1)$, and $\hat{J}_z = \frac{1}{2}(\hat{a}_1^\dagger \hat{a}_1 - \hat{a}_2^\dagger \hat{a}_2)$. With the ladder operators $\hat{J}_+ = \hat{J}_x + i\hat{J}_y$ and $\hat{J}_- = \hat{J}_x - i\hat{J}_y$ the Hamiltonian (1) becomes

$$\hat{H} = 2U\hat{J}_z^2 + 2\delta\hat{J}_z - T(\hat{J}_+ + \hat{J}_-) + \tfrac{1}{2}U\hat{N}^2 - U\hat{N}, \tag{3}$$

where $\hat{N}$ is the total particle number operator. For fixed N a change from basis $|n, N-n\rangle$ to the angular momentum states $|l, j\rangle$ is useful, with $l = N/2$ and $j = (n_1 - n_2)/2$. With $w_j = 2Ul^2 - 2Ul + 2Uj^2 + 2\delta j$ and $p_j = -T\sqrt{l(l+1) - j(j-1)}$, the eigenvalues of the Hamiltonian are determined by an equation of the form

$$p_j c_{j-1} + (w_j - E)c_j + p_{j+1}c_{j+1} = 0, \tag{4}$$

as discussed in Ref. [18]. By introducing the "coordinate" operator $\phi = i\frac{\partial}{\partial j}$ (note Ref. [19]), Eq. (4) can be written as a Schrödinger equation for the function c_j with eigenvalue E and Hamilton operator $\hat{H} = w(j) + p(j)e^{-i\phi} + p(j+1)e^{i\phi}$. In the classical limit the operators turn to canonically conjugate coordinate ϕ and momentum j (population imbalance), where ϕ turns out to be the phase difference between the two wells. Since $p(j)$ is a slowly varying function of j in the classical limit ($N \to \infty$) one can replace both p_j and p_{j+1} by $p_{j+\frac{1}{2}}$ and one finds the Hamilton function

$$H(j,\phi) = w(j) + 2p\left(j + \frac{1}{2}\right)\cos\phi \tag{5a}$$

$$= \frac{1}{2}UN^2 - UN + 2Uj^2 + 2\delta j - 2T\sqrt{(N/2)^2 - j^2}\cos\phi, \tag{5b}$$

which can also be found from the mean-field Gross-Pitaevskii functional in the two-mode limit [17,20]. The classical dynamics of the population imbalance and the relative phase (for $\delta = 0$) is then determined by Hamilton's equations of motion:

$$\frac{dj}{dt} = -\frac{\partial H}{\partial \phi} = -2T\sqrt{(N/2)^2 - j^2}\sin\phi,$$
$$\frac{d\phi}{dt} = \frac{\partial H}{\partial j} = 4Uj + \frac{2Tj\cos\phi}{\sqrt{(N/2)^2 - j^2}}. \tag{6}$$

The rich dynamics in this "classical picture" have been studied by several groups [14,21,22], focusing on the differences between the classical and the quantum description of the dynamics [23–25]. Clearly a purely classical description cannot picture the collapses and the revivals of the population imbalance, but it is able to shed light on the transition from the tunneling to the self-trapping regime. Recently, the phase space region near the classical bifurcation was also investigated experimentally with ultracold bosons [26].

A. Semiclassical energy spectrum: Bohr-Sommerfeld quantization

An analytical approach to the energy spectrum relies on the WKB method following Braun [18] and others [6–9]. In Ref. [6], only the noninteracting case is investigated analytically. In Refs. [8,9] the authors concentrate on energies close to the extremal points, and in Ref. [7] the case of an attractive gas for the single value of $\Lambda = 1$ is studied. We here concentrate on the plasma oscillating regime and aim for solutions over the whole range of $\Lambda \ll 1$ to $\Lambda \gg 1$.

For the Hamilton function (5b) it is convenient to introduce two potential-energy curves

$$V^+(j) = H(j,\pi) = TN + 2Uj^2 + 2T\sqrt{(N/2)^2 - j^2}, \quad (7)$$

$$V^-(j) = H(j,0) = TN + 2Uj^2 - 2T\sqrt{(N/2)^2 - j^2}, \quad (8)$$

such that the classically allowed energies lie in the region confined by the two potential curves V^+ and V^-. The minimum energy is chosen to be $V^-(j=0) = 0$. The potential curves display the transition from the Rabi regime to the Josephson regime very nicely, as shown in Fig. 1. The energy eigenvalues change from a (non-harmonic) oscillator like spectrum for $\Lambda < 1$ to a spectrum with doublets for $\Lambda > 1$ due to tunneling, which can be seen from the potential curves. For $\Lambda > 1$, V^+ attains a local minimum which leads to doublets in the spectrum for energies $E > V^+(0)$. The deeper the minimum, the bigger this so-called Fock fraction of the spectrum. Since we are interested in plasma oscillations, the Fock fraction will not be investigated here, but a semiclassical analysis along similar lines—if only more involved—is possible; see, for instance, Ref. [27].

In the WKB approximation the eigenenergies E_n are obtained from the quantization condition

$$S = S(E) = \oint \phi(j)dj = 4\int_0^{j_+(E)} \arccos \times \left(\frac{E - TN - 2Uj^2}{2T\sqrt{(N/2)^2 - j^2}}\right) dj = 2\pi\left(n + \frac{1}{2}\right), \quad (9)$$

where n is the quantum number and $\phi(j)$ is determined by the Hamilton function (5b) at fixed energy E [recall that zero energy $E = 0$ corresponds to $S(E=0) = 0$]. The integration limit j_+ is the (positive) classical turning point as obtained from

$$\sqrt{[V^+(j) - E][E - V^-(j)]} \stackrel{!}{=} 0, \quad (10)$$

which leads to a quadratic equation in j^2 with solutions

$$(j^2)_\pm(E) = \frac{1}{2U^2}\Big\{[EU - (\omega_p/2)^2] \pm \sqrt{(\omega_p/2)^4 - EU\omega_p^2/[2(1+\Lambda)]}\Big\}. \quad (11)$$

Recall that $\omega_p = 2T\sqrt{1+\Lambda}$ is the plasma frequency. For the plasma oscillating regime the relevant turning point is j_+. Note that $j_+ \to 0$ for $E \to 0$, while (j_-^2) approaches the negative constant $(j_-^2) \to -[\omega_p/(2U)]^2$ as $E \to 0$.

The integral in Eq. (9) can be solved numerically and the results agree very well with the exact quantum results even for quite small numbers of particles, as has already been noticed in Ref. [6]. We are unaware of a simple analytical expression for the action integral. Because we aim for the plasma oscillation regime, we expand in powers of E. First, however, we take the derivative with respect to energy and rescale to find

$$\frac{\partial S(E)}{\partial E} = \frac{2}{U|j_-(E)|}\int_0^1 \frac{d\lambda}{\sqrt{(1-\lambda^2)[1+\kappa^2(E)\lambda^2]}}. \quad (12)$$

with $\kappa^2 = (j_+)^2/|j_-|^2$. Since $\kappa^2 \to 0$ for $E \to 0$, and $0 < \lambda < 1$, an expansion of $(1+\kappa^2\lambda^2)^{-1/2}$ in powers of $\kappa^2\lambda^2$ leads to a series in powers of E. The corresponding integrals $\int_0^1 d\lambda\lambda^{2n}/\sqrt{1-\lambda^2}$ are known analytically. Finally, a systematic expansion of κ^{2n} and $1/|j_-|$ in E leads to

$$\frac{\partial S}{\partial E} = \frac{2\pi}{\omega_p} + 4\pi\frac{U(1+\Lambda/4)}{\omega_p^3(1+\Lambda)}E + 6\pi\frac{3U^2[1+\Lambda/3+(\Lambda/4)^2]}{\omega_p^5(1+\Lambda)^2}E^2 + \cdots, \quad (13)$$

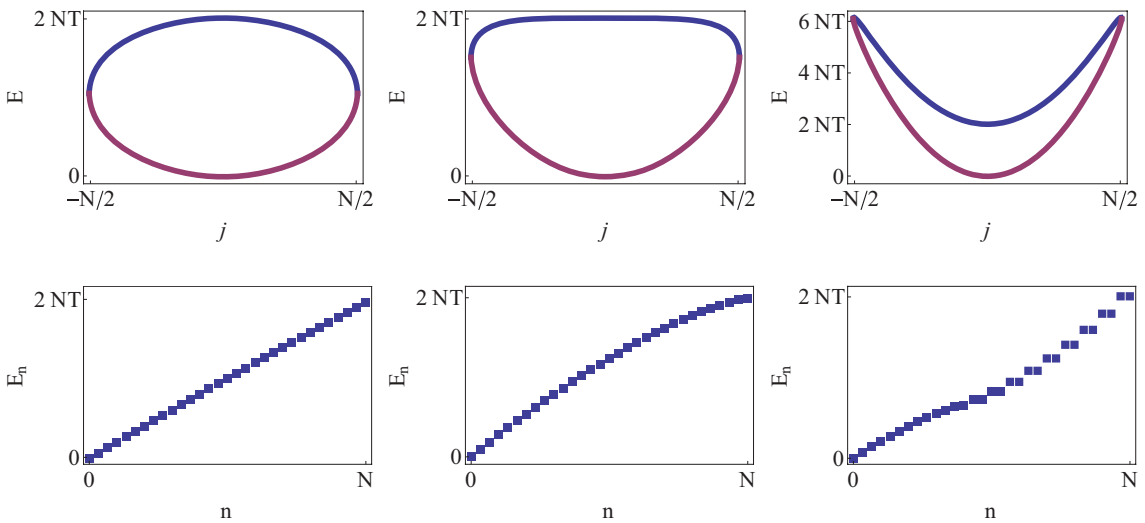

FIG. 1. (Color online) Potential curves V^+, V^- and the energy eigenvalues E_n for, from left to right, $\Lambda = 0.1$, 1, 10 and $N = 30$, $T = 3$.

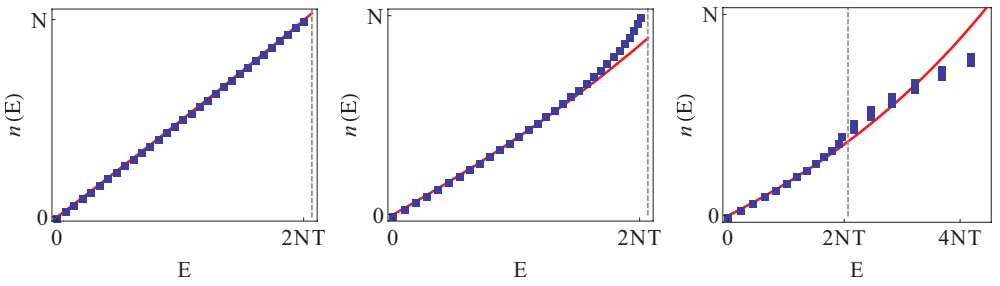

FIG. 2. (Color online) Comparison of the analytical (15) (red, solid line, including third order in E) and the numerically exact spectrum (blue squares) for, from left to right, $\Lambda = 0.1, 1, 10$ and for $N = 30$, $T = 3$. The vertical dashed lines illustrate the transition from the plasma oscillating regime to the self-trapping regime at $E = V^+(0) = 2NT$. We see excellent agreement in the plasma oscillating regime.

which is one of the important results of this paper. Apparently, the formal expansion in E is an expansion in the dimensionless parameter

$$\varepsilon = \frac{UE}{\omega_p^2} = \frac{1}{2}\frac{\Lambda}{1+\Lambda}\left(\frac{E}{V^+(0)}\right). \tag{14}$$

The expression on the right-hand side clearly shows that our results are expected to be valid in the plasma oscillating regime $E < V^+(0)$, irrespective of the value of Λ. From a simple integration together with the Bohr-Sommerfeld-quantization condition (9) we find

$$n(E) = -\frac{1}{2} + \frac{1}{\omega_p}E + \frac{U(1+\Lambda/4)}{\omega_p^3(1+\Lambda)}E^2 + \frac{3U^2[1+\Lambda/3+(\Lambda/4)^2]}{\omega_p^5(1+\Lambda)^2}E^3 + \cdots. \tag{15}$$

In Ref. [12] the inverse expansion $E(n)$ up to second order in n is considered, which is in agreement with Eq. (15) in the corresponding orders. In Fig. 2 we show examples of the spectrum for a wide range of values of $\Lambda = 0.1, 1, 10$, covering both the Rabi and the Josephson regime. Apparently, our approximation (15), including contributions up to third order in E, coincides with the numerically exact spectrum with high accuracy in the plasma oscillating regime [$E < V^+(0)$] for all values of Λ. Clearly, the doublet structure in the Fock regime [high-energy regime $E > V^+(0)$ in the right diagram of Fig. 2] cannot be captured by our series expansion (15).

III. EXACT QUANTUM DYNAMICS OF POPULATION IMBALANCE

To determine the tunneling dynamics, the Bose-Hubbard Hamiltonian (1) can be diagonalized numerically for a finite number of bosons. Using the eigenbasis $\{|\phi_n\rangle\}$, the dynamics of $|\psi(t)\rangle$ is given by

$$|\psi(t)\rangle = \sum_n c_n e^{-iE_n t}|\phi_n\rangle, \quad \text{with } c_n = \langle\phi_n|\psi_0\rangle. \tag{16}$$

The time evolution of the population imbalance $\hat{j} = (\hat{n}_1 - \hat{n}_2)/2$ is then

$$j(t) = \langle\psi(t)|\hat{j}|\psi(t)\rangle = \sum_{n,m} A_{nm} e^{-i(E_n - E_m)t}, \tag{17}$$

with the matrix

$$A_{nm} = c_n c_m^* \langle\phi_m|\hat{j}|\phi_n\rangle. \tag{18}$$

The dynamics of the population imbalance thus depends on the energy spectrum through the differences $E_n - E_m$, and on the matrix A_{nm}, which contains the initial condition and matrix elements $\langle\phi_m|\hat{j}|\phi_n\rangle$.

Figure 3 shows the matrix A_{nm} for increasing Λ, obtained from a numerically exact calculation.

Due to parity with respect to $\hat{j}$, A_{nm} is zero for an even number $n - m$, as can be seen in Fig. 3: $0 = A_{nn} = A_{nn\pm2} = A_{nn\pm4} + \cdots$. Among the nonzero matrix elements, there is a strong hierarchy,

$$|A_{nn\pm1}| \gg |A_{nn\pm3}| \gg |A_{nn\pm5}| \gg \cdots, \tag{19}$$

in particular for small Λ, which will be important later. It is worth noting that in the limit $U \to 0$ (and therefore $\Lambda \to 0$,

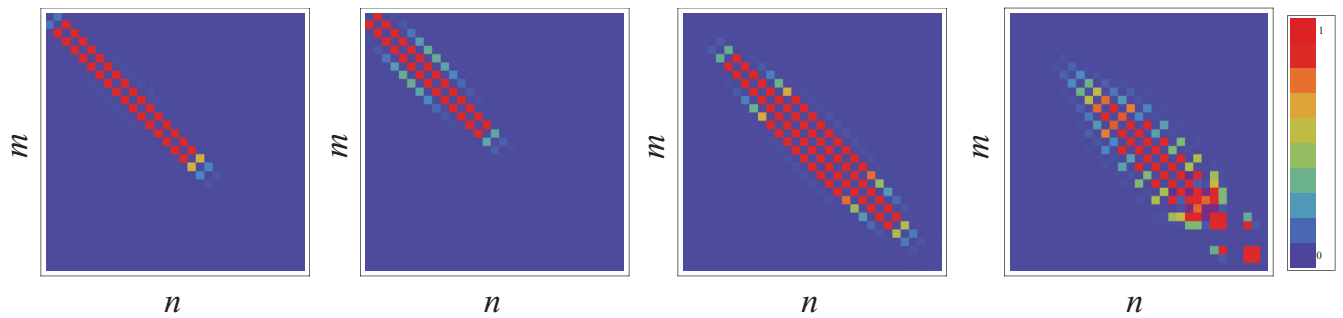

FIG. 3. (Color online) Matrix A_{nm} for $\Lambda = 0.1, 0.5, 1, 10$ and for $N = 30$, $T = 3$.

for fixed N) the dynamics is well described by a harmonic oscillator. In that case it is easy to prove [the $\phi_n(j)$ are Hermite polynomials] that only the $A_{nn\pm1}$ are in fact different from zero.

Along the diagonals, the matrix elements $A_{nn\pm k}$ (with $k = 1, 3, 5, \ldots$) have a Gaussian-like n dependence. This is due to the n dependence of the overlap $c_n = \langle\phi_n|\psi_0\rangle$, which will be discussed in the next section. By contrast, the n dependence of the matrix elements $\langle\phi_{n\pm k}|\hat{j}|\phi_n\rangle$ is weak. Thus, it is safe to assume the form

$$A_{nn\pm k} \approx c_n c^*_{n\pm k} d_k, \tag{20}$$

with n-independent parameters $d_k \approx \langle\phi_{\bar{n}\pm k}|\hat{j}|\phi_{\bar{n}}\rangle$ (with the most relevant being $\bar{n}$) for which, following Eq. (19), we expect

$$|d_1| \gg |d_3| \gg |d_5| \gg \cdots. \tag{21}$$

IV. SEMICLASSICAL DYNAMICS OF POPULATION IMBALANCE

For a semiclassical evaluation of $j(t)$ according to Eqs. (17) and (18) we need semiclassical expressions for $E_n - E_{n\pm k}$ and the overlap coefficients c_n. While the spectrum was discussed in Sec. II, we start here with the latter.

A. Reflection principle

The problem to find overlap integrals of an initial wave packet $\psi_0(j)$ localized near $j \approx j_0$ with eigenstates $|\phi_E\rangle$ of the Hamiltonian with potential $V(j) = V^-(j)$ is often encountered in molecular photodissociation [28]. The semiclassical solution (reflection principle) states that

$$\langle\phi_E|\psi_0\rangle = c\psi_0\left(\frac{E - V(j_0)}{V'(j_0)}\right), \tag{22}$$

with some constant c. It is important to note that here the eigenstates are understood to be energy normalized [i.e., $\langle\phi_E|\phi_{E'}\rangle = \delta(E - E')$], since in typical applications these are scattering states. For the coefficients c_n we therefore find $c_n = \langle\phi_n|\psi_0\rangle = \sqrt{\frac{dE}{dn}}\langle\phi_E|\psi_0\rangle$. The normalization condition $1 = \sum_n |c_n|^2 \approx \int dn|c_n|^2$ yields $c = 1/\sqrt{V'(j_0)}$, and we get

$$c_n = \langle\phi_n|\psi_0\rangle \approx \frac{1}{\sqrt{V'(j_0)}}\sqrt{\frac{dE(n)}{dn}}\psi_0\left(\frac{E_n - V(j_0)}{V'(j_0)}\right). \tag{23}$$

In our calculations, following the experiments, the initial wave function is prepared as the ground state of the tilted trap potential [achieved through the term $\delta(\hat{n}_1 - \hat{n}_2) = 2\delta\hat{j}$ in the Bose-Hubbard Hamiltonian (1)]. In a harmonic approximation near the potential minimum of the tilted potential we find the Gaussian density

$$|\psi_0(j)|^2 = \frac{1}{\sqrt{2\pi\sigma^2}}\exp\left[-\frac{(j - j_0)^2}{2\sigma^2}\right], \tag{24}$$

with j_0 uniquely determined by the tilting strength δ and

$$\sigma^2 = \frac{N}{4}\frac{1 - (2j_0/N)^2}{\sqrt{1 + \Lambda[1 - (2j_0/N)^2]^{3/2}}}. \tag{25}$$

Clearly, the shape of the initial wave function determines the shape of the c_n as a function of n. On closer inspection of Eq. (23), however, we observe that for the initial state (24), due to the nonlinear relation between E_n and n, the coefficients c_n are gaussian in E_n but not in n.

B. Population imbalance

Having all the ingredients at hand we can now aim at a semiclassical expression for the dynamics of the population imbalance $j(t)$ which we choose to write as

$$j(t) = \sum_{n,k} A_{nn-k}\exp[-i(E_n - E_{n-k})t] + \text{c.c.}, \tag{26}$$

with $k = 1,3,5,\ldots$ taking into account the diagonal structure of A_{nm} as discussed in the last section. Replacing $A_{nn\pm k}$ by expression (20) and using the Poisson summation formula we find

$$j(t) = \sum_{k=1,3,5,\ldots} d_k \sum_{m=-\infty}^{\infty} I^k_m(t) + \text{c.c.}, \tag{27}$$

with

$$I^k_m(t) = \int dn\left(\frac{dE}{dn}\right)\frac{1}{V'(j_0)}\psi_0\left(\frac{E_n - V(j_0)}{V'(j_0)}\right)\psi^*_0 \times\left(\frac{E_{n-k} - V(j_0)}{V'(j_0)}\right)e^{-i(E_n - E_{n-k})t}e^{2\pi imn}. \tag{28}$$

This rather complicated expression is readily simplified by changing the integration variable from n to E. Further, as only very small k ($k = 1,3$) are relevant [see Eq. (21)], it is safe to replace $E_n - E_{n-k} \approx \frac{dE}{dn}k = 2\pi k/S'(E)$ and neglect the k dependence in the reflection principle (i.e., $c^*_{n\pm k} \approx c^*_n$). Finally, we replace $2\pi n = S(E) - \pi$ according to the semiclassical quantization rule (9). With $\tau = kt$ we find

$$I^k_m(t) = I_m(\tau) = e^{i\pi m}\int\frac{dE}{V'(j_0)}\left|\psi_0\left(\frac{E - V(j_0)}{V'(j_0)}\right)\right|^2 \times e^{-2\pi i\tau/S'(E)}e^{imS(E)}. \tag{29}$$

This expression, together with Eq. (27), is one of the main results of our paper. As we will see, even with further simplifications, the formula captures all essential details of the dynamics, allows for a thorough understanding of decay and revival dynamics, and, most importantly, is the starting point for analytical expressions.

Due to the localization of the initial state $\psi_0(j)$, the energy integration in Eq. (29) is confined to a relatively small interval near $E \approx V(j_0)$, which we assume to be in the plasma oscillating regime [$E < V^+(0)$]. Therefore, for the evaluation of the overall phase $mS(E) - 2\pi kt/S'(E)$ we can rely on our semiclassical series expansions (13) and (15). With a Gaussian initial state as in Eq. (24) and expanding the overall phase up to second order around $E \approx V(j_0)$ allows us to take the Gaussian integral and leads us to the analytical result

$$I_m(\tau) + \text{c.c.} = \frac{2}{(1 + A^2)^{1/4}}\cos(\tilde{\omega}_p\tau - \tilde{\varphi}) \times\exp\left[-\frac{1}{2(1 + A^2)}\left(\frac{\tau - mT_{\text{rev}}}{T_{\text{collapse}}}\right)^2\right], \tag{30}$$

with $\tau = kt$. In the following we want to discuss the structure of this central result. The most important features are the

plasma oscillations ($\tilde{\omega}_p$), their collapse (T_{collapse}), and their revivals (T_{rev}).

The phase $\tilde{\varphi} = \tilde{\varphi}(\tau, m)$ can be ignored for a qualitative discussion—it is a complicated expression and can be found in the Appendix. Importantly, $\tilde{\varphi}$ varies slowly with time and thus needs only to be taken into account when quantitative agreement with exact calculations over extremely long time scales is sought.

The parameter $A = A(\tau, m) = \tau\Sigma_\tau - m\Sigma_m$ (expressions for the constants Σ_τ and Σ_m can be found in the Appendix) describes an additional slow broadening and decay of the signal. As for the phase $\tilde{\varphi}$, the inclusion of A leads to quantitative agreement with exact calculations as shown later, but need not be discussed further here.

Thus we concentrate on the important plasma oscillations ($\tilde{\omega}_p$), their collapse (T_{collapse}), and their revivals (T_{rev}).

The analytical formula for the generalized plasma frequency for arbitrary Λ is

$$\tilde{\omega}_p = \omega_p(1 - 2c_1 g - 5c_2 g^2), \tag{31}$$

which is valid both in the Rabi and the Josephson regime. Here, $c_1 = (1 + \Lambda/4)/(1 + \Lambda)$ and $c_2 = (1 + \Lambda/5 + \Lambda^2/4^2)/(1 + \Lambda)^2$ are Λ-dependent numbers of order unity and $g = UV(j_0)/\omega_p^2$ is a dimensionless interaction parameter. We give a more elaborate discussion of this expression in Sec. VI.

For the revival time we find

$$T_{\text{rev}} = \frac{\pi}{U}\frac{(1 + 2c_1 g)}{(c_1 + 5c_2 g)}, \tag{32}$$

and for the collapse time

$$T_{\text{collapse}} = \frac{1}{2g\,\Delta V_0\,\omega_p(c_1 + 5c_2 g)}, \tag{33}$$

with

$$\Delta V_0 = \sigma V'(j_0)/V(j_0) \tag{34}$$

being the width of the wave packet in energy in units of the mean excited energy. Again, a more elaborate discussion of these results will be given in Sec. VI.

C. Simple Rabi limit

In the well-studied Rabi limit (i.e., when $\Lambda \ll 1$), our results simplify. In particular, $\tilde{\omega}_p \to \omega_p$, $T_{\text{rev}} \to \pi/U$, and $T_{\text{collapse}} \to (2g\Delta V_0\omega_p)^{-1}$. Moreover, only the main off-diagonal contribution $k = 1$ of the matrix $A_{nn\pm k}$ needs to be taken into account. Thus, in the Rabi limit, the dynamics of the population imbalance is governed by the simple expression

$$j(t) = j_0 \sum_m \cos(\omega_p t)\exp\left[-2\omega_p^2 g^2 (\Delta V_0)^2\left(t - \frac{\pi m}{U}\right)^2\right]; \tag{35}$$

a result that with an appropriate identification of the parameters can also be found in the literature [29].

V. COMPARISON OF RESULTS

Equation (30) describes the dynamics of the population imbalance without any free parameter. The population imbalance oscillates with the generalized plasma frequency $\tilde{\omega}_p$, with roughly a Gaussian envelope of width T_{collapse} (note that the parameter A contributes to the envelope, in particular for long times). The sum over m counts the revivals—the initial collapse dynamics is captured by $m = 0$, the first revival corresponds to the contribution of $m = 1$, and so on. The sum over k takes into account further off-diagonal contributions in the matrix $A_{nn\pm k}$ which lead to small revivals (of the order of d_k) at earlier times mT_{rev}/k with k-fold frequency. For $\Lambda = 25$, for instance, one can see tiny contributions of $k = 3$ at one third and two thirds of the full revival time in Fig. 7.

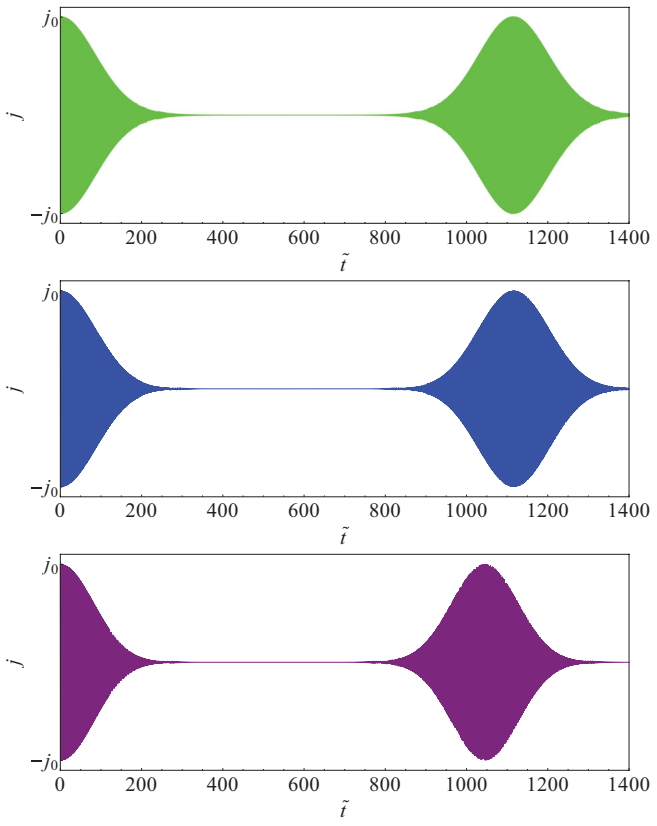

FIG. 4. (Color online) Comparison of exact dynamics (top) of population imbalance j with improved semiclassical expression (30) (middle) and expression for Rabi limit (35) (bottom) as a function of dimensionless time $\tilde{t} = \tilde{\omega}_p t/(2\pi)$ for $\Lambda = 0.1$, $T = 10$, $N = 100$, and an initial $j_0 = 20$.

Figures 4–7 show a comparison of the exact dynamics of the population imbalance, our analytical expression (30) (taking into account $k = 1$ only), and the simple expression for the Rabi limit (35), for different values of Λ between 0.1 and 25.

Obviously, our semiclassical expression (30) describes the exact dynamics almost perfectly over this huge range of values of Λ. By contrast, the simple expression (35) is valid, indeed, for only very small values of Λ ($\Lambda = 0.1$), as expected. For increasing Λ the simple Rabi expression fails, as can be seen from Figs. 5 and 6.

VI. DISCUSSION

Having an analytical expression for the time evolution of the population imbalance allows us to discuss the dependence

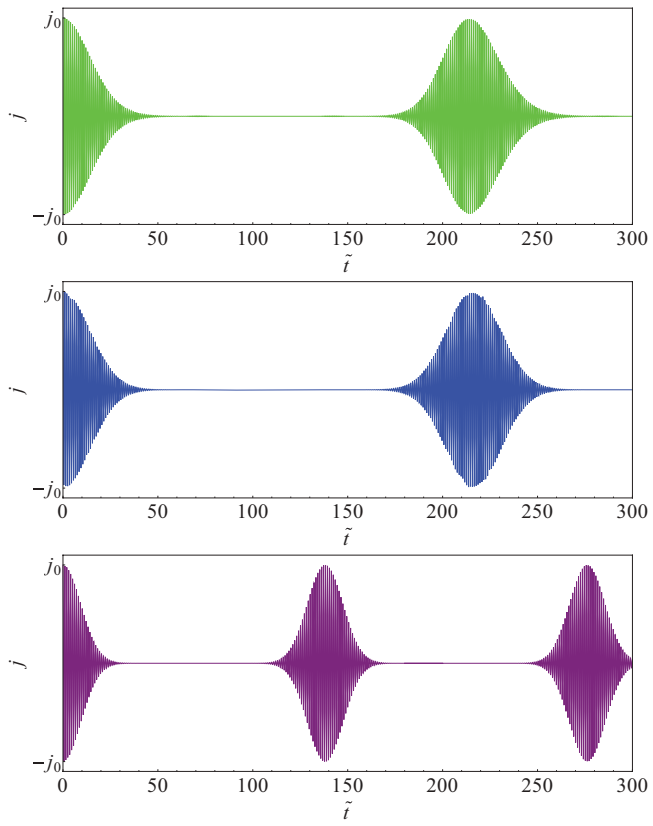

FIG. 5. (Color online) Comparison of exact dynamics (top) of population imbalance j with improved semiclassical expression (30) (middle) and expression for Rabi limit (35) (bottom) as a function of dimensionless time $\tilde{t} = \tilde{\omega}_p t/(2\pi)$ for $\Lambda = 1$, $T = 10$, $N = 100$, and an initial $j_0 = 20$.

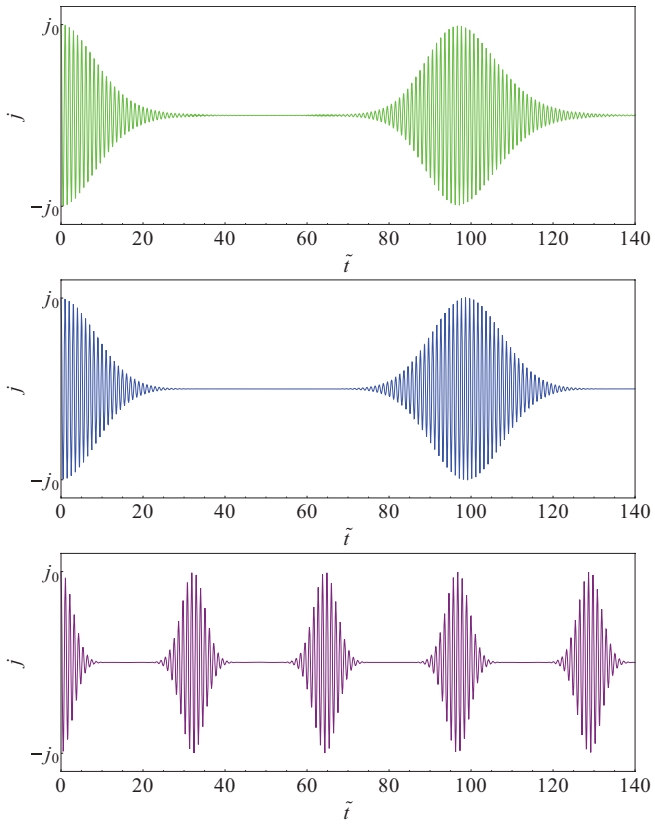

FIG. 6. (Color online) Comparison of exact dynamics (top) of population imbalance j with improved semiclassical expression (30) (middle) and expression for Rabi limit (35) (bottom) as a function of dimensionless time $\tilde{t} = \tilde{\omega}_p t/(2\pi)$ for $\Lambda = 10$, $T = 10$, $N = 100$, and an initial $j_0 = 10$.

of the collapse and revival time and the plasma oscillation frequency on the relevant parameters of the system.

A. Plasma oscillation frequency

The plasma oscillation frequency was found to be

$$\tilde{\omega}_p = \omega_p(1 - 2c_1 g - 5c_2 g^2), \tag{36}$$

with $c_1 = (1 + \Lambda/4)/(1 + \Lambda)$, $c_2 = (1 + \Lambda/5 + \Lambda^2/4^2)/(1 + \Lambda)^2$, and $g = UV(j_0)/\omega_p^2$. For very small Λ, the correct $\tilde{\omega}_p$ approaches the standard plasma frequency ω_p, since the constants c_1 and c_2 tend to unity in this limit, and the parameter g approaches zero: with $V(j_0) \approx \omega_p^2 j_0^2/(2NT)$ (harmonic approximation of the potential), it is worth writing the latter parameter in the form

$$g \approx \frac{\Lambda}{8}(2j_0/N)^2, \tag{37}$$

which shows that g tends to zero linearly in Λ for fixed initial imbalance (j_0/N). However, for increasing Λ the correction terms in $\tilde{\omega}_p$ becomes more and more relevant, especially for large j_0, as can be seen from Eq. (37). Figure 8 shows a comparison of the plasma frequency obtained from numerically exact results and the semiclassical expression (31) as a function of Λ for different initial imbalance j_0. It can be seen that the classical plasma frequency ω_p is only a good approximation for very small Λ, as expected. Especially for relatively large initial imbalance $j_0 = 20$ with $N = 100$, the numerically exact plasma frequencies (circles) differ strongly from ω_p, but are in very good agreement with the new semiclassical expression $\tilde{\omega}_p$ (blue, solid line). Since $\Lambda = 25$ and an initial $j_0/N \approx 0.15$ are typical experimental values [2], this discrepancy becomes by all means relevant. Sure enough, with the parameters given in Ref. [2], our formula leads to $2\pi/\tilde{\omega}_p = 39$ ms, which is the experimentally observed value. By contrast, without our corrections one would find $2\pi/\omega_p = 30$ ms.

B. Collapse time

According to Eq. (30), the collapse time is given by

$$T_{\text{collapse}} = \frac{1}{2g\Delta V_0 \omega_p (c_1 + 5c_2 g)}. \tag{38}$$

The expression in front of the brackets (which can be identified with the collapse time in the Rabi regime; i.e., for small Λ) can be approximated as $N/[\Lambda\omega_p(2j_0/N)]\sigma$. Thus, assuming Λ and (j_0/N) are kept fixed so that σ is proportional to $\sqrt{N}$, the collapse time is proportional to $\sqrt{N}$. This $\sqrt{N}$ behavior has been stated before in Refs. [7,30]. Our semiclassical formula shows, however, that this statement is only correct for the special case of fixed Λ and j_0/N, or in the Rabi limit ($\Lambda \ll 1$). In all the other cases, the collapse time depends in a nontrivial

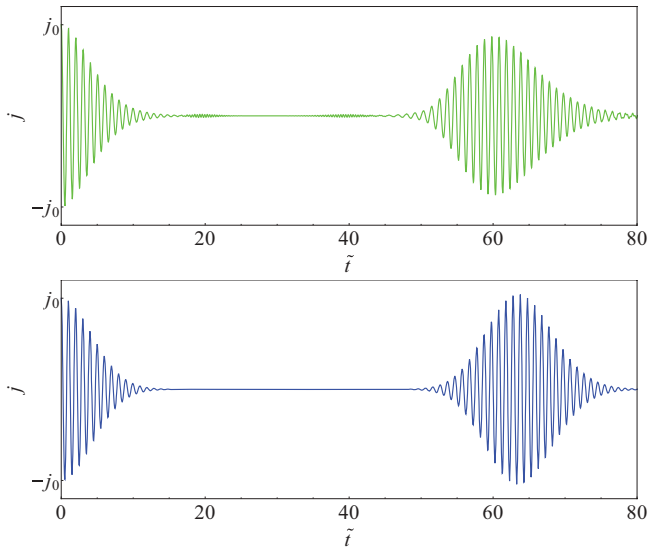

FIG. 7. (Color online) Comparison of exact dynamics (top) of population imbalance j with improved semiclassical expression (30) (bottom) as a function of dimensionless time $\tilde{t} = \tilde{\omega}_p t/(2\pi)$ for $\Lambda = 25$, $T = 10$, $N = 100$, and an initial $j_0 = 10$.

way on N through Λ and j_0/N. Figures 4–7, and in detail Fig. 9, show that our semiclassical expression for the collapse time is remarkably reliable.

C. Revival time

Following Eq. (30), the revival time is

$$T_{\rm rev} = \frac{\pi}{U}\frac{(1+2c_1 g)}{(c_1+5c_2 g)}. \tag{39}$$

Most interestingly, in the Rabi limit it becomes independent of the number of particles and in fact independent of any other system parameter except the interaction strength U. The revival time was already discussed in Ref. [25] where

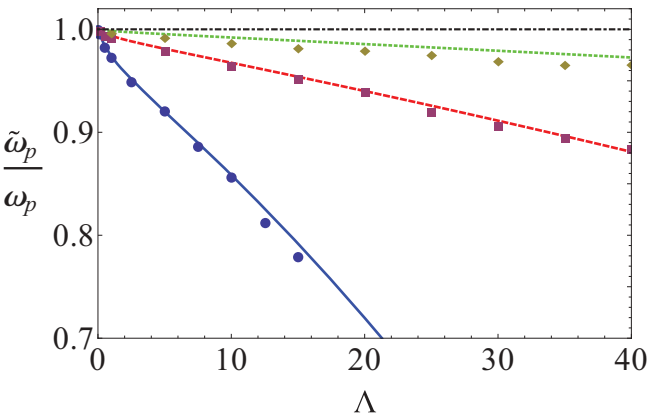

FIG. 8. (Color online) Comparison of numerically exact (symbols) and improved semiclassical analytical (31) (lines) plasma oscillation frequency as a function of Λ for different j_0. $j_0 = 5$ (diamonds, dotted line), $j_0 = 10$ (squares, dashed line), $j_0 = 20$ (circles, solid line), for a total number of $N = 100$ particles. The constant dash-dotted line indicates the simple plasma frequency ω_p, valid only in the Rabi regime $\Lambda \ll 1$.

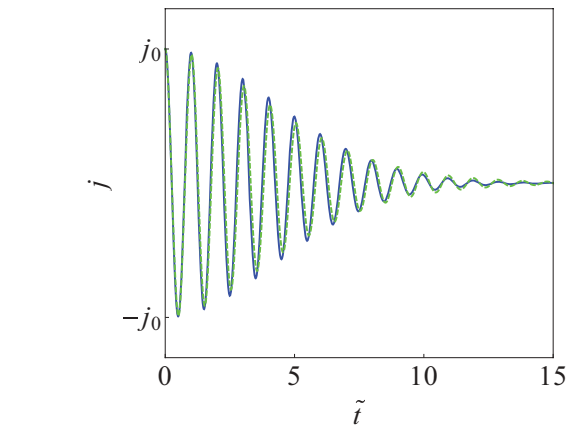

FIG. 9. (Color online) Detailed comparison of numerical exact initial collapse dynamics of j (green, dashed line) and improved semiclassical analytical results (blue, solid line) for $\Lambda = 25$, $N = 100$, $T = 10$, and $j_0 = 10$ as a function of dimensionless time $\tilde{t} = \tilde{\omega}_p t/(2\pi)$.

it was found to be equal to 4π, with an interaction strength of $1/4$ (considering the different definition of parameters), which we confirm here, in the Rabi limit. Furthermore, it is stated in Refs. [7,25] that the revival time grows linearly with the number N of particles. This is obviously true for those investigations with $UN = \text{const}$ only, as can be seen from our expression (39). However, note that even only slightly away from the Rabi limit, when Λ approaches or becomes greater than unity, the constants c_1 and c_2 and the parameter g become relevant. This can be seen from Fig. 10. Thus, for $\Lambda > 1$ no simple scaling law for the revival time exists.

The figure shows that for increasing Λ the exact revival times differ strongly from the revival time π/U predicted by the Rabi-limit formula. On the other hand, it can be seen that the improved semiclassical expression (39) reproduces the exact revival times very nicely even for $\Lambda > 1$. For increasing values of Λ the self-trapping fraction of the phase space is

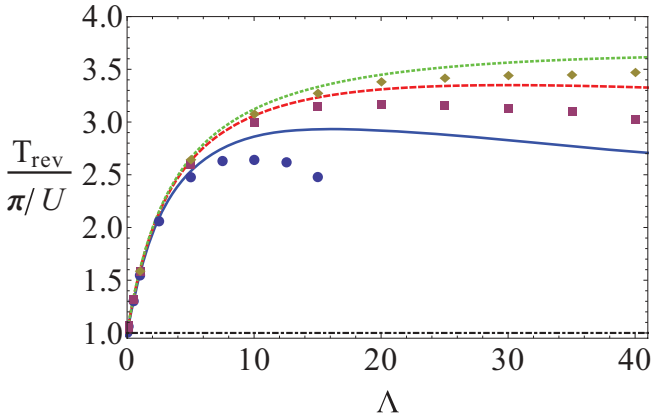

FIG. 10. (Color online) Comparison of numerically exact (symbols) and improved semiclassical analytical revival time (lines) as a function of Λ for different initial imbalance j_0. $j_0 = 5$ (diamonds, dotted line), $j_0 = 10$ (squares, dashed line), $j_0 = 20$ (circles, solid line), for a total number of $N = 100$ particles. The dashed-dotted line indicates the result π/U of the Rabi limit, which is obviously only valid for very small Λ.

increasing as well, such that for large initial excitations (e.g., $j_0 = 20$ for $N = 100$), the semiclassical analysis ceases to give reliable results.

VII. CONCLUSION

We applied semiclassical methods to the well-known two-mode Bose-Hubbard model in order to investigate in detail Bose-Einstein condensate (BEC) tunneling in a double-well trap. Within the plasma oscillation regime we found analytical expressions for the energy spectrum and the initial state that agrees nicely with numerically exact results. Employing the reflection principle and the Poisson summation formula led us to an analytical expression for the time evolution of the population imbalance of the Bose gas in the double well. This allows us to discuss the dependence of characteristic quantities of the dynamics, like plasma oscillation frequency and collapse and revival times on the relevant system parameters. Our results thus provide a detailed understandingof the two-mode model. Finally, our generalized formula for the plasma oscillation frequency agrees perfectly well with experimental findings. Challenging as it may be, we hope that our predictions for collapse and revival times will be confirmed experimentally, too.

Semiclassical methods are well suited to study nonequilibrium dynamics of a bosonic interacting many-body quantum system. For systems with more degrees of freedom, an explicitly time-dependent approach might prove useful.

ACKNOWLEDGMENTS

We thank Markus Oberthaler for a nice discussion. L.S. acknowledges support from the International Max Planck Research School (IMPRS), Dresden.

APPENDIX: PARAMETERS

In order to complete the discussion of our semiclassical analytical result for the time evolution of the population imbalance (30), we present here the definition of the remaining parameters. The phase of the oscillation reads

$$\tilde{\varphi} = -m\varphi_m + \frac{1}{2}\arctan A - \frac{A}{2(1+A^2)}\left(\frac{\tau - mT_{\mathrm{rev}}}{T_{\mathrm{collapse}}}\right)^2, \tag{A1}$$

where the dominantly m-dependent part is defined separately as

$$\varphi_m = 2\pi\bar{V}[1 + c_1 g - 1/(2\bar{V})]. \tag{A2}$$

$\bar{V}$ is the mean excited energy in units of the plasma frequency

$$\bar{V} = V(j_0)/\omega_p. \tag{A3}$$

Furthermore, the quantity

$$A = \tau\Sigma_\tau - m\Sigma_m \tag{A4}$$

contributes to an overall slow spread and decay of the signal. It can be separated in a τ- and a m-dependent contribution with

$$\Sigma_\tau = 10c_2(\Delta V_0)^2 g^2 \omega_p \tag{A5}$$

and

$$\Sigma_m = 4\pi c_1(\Delta V_0)^2 g\bar{V}. \tag{A6}$$

For completeness, we repeat the expressions

$$c_1 = \frac{(1+\Lambda/4)}{(1+\Lambda)}, \quad c_2 = \frac{(1+\Lambda/5+\Lambda^2/4^2)}{(1+\Lambda)^2},$$
$$g = \frac{UV(j_0)}{\omega_p^2}, \quad \Delta V_0 = \frac{\sigma V'(j_0)}{V(j_0)},$$

from Sec. IV B.

[1] M. Albiez, R. Gati, J. Fölling, S. Hunsmann, M. Cristiani, and M. K. Oberthaler, Phys. Rev. Lett. **95**, 010402 (2005).
[2] R. Gati and M. K. Oberthaler, J. Phys. B: At., Mol. Opt. Phys. **40**, R61 (2007).
[3] A. Vardi and J. R. Anglin, Phys. Rev. Lett. **86**, 568 (2001).
[4] J. R. Anglin and A. Vardi, Phys. Rev. A **64**, 013605 (2001).
[5] K. W. Mahmud, H. Perry, and W. P. Reinhardt, Phys. Rev. A **71**, 023615 (2005).
[6] E. M. Graefe and H. J. Korsch, Phys. Rev. A **76**, 032116 (2007).
[7] K. Pawlowski, P. Zin, K. Rzazewski, and M. Trippenbach, Phys. Rev. A **83**, 033606 (2011).
[8] R. Franzosi, V. Penna, and R. Zecchina, Int. J. Mod. Phys. B **14**, 943 (2000).
[9] M. Chuchem, K. Smith-Mannschott, M. Hiller, T. Kottos, A. Vardi, and D. Cohen, Phys. Rev. A **82**, 053617 (2010).
[10] V. S. Shchesnovich and M. Trippenbach, Phys. Rev. A **78**, 023611 (2008).
[11] F. Nissen and J. Keeling, Phys. Rev. A **81**, 063628 (2010).
[12] A. P. Itin and P. Schmelcher, Phys. Rev. A **84**, 063609 (2011).
[13] A. Leggett, Rev. Mod. Phys. **73**, 307 (2001).
[14] G. J. Milburn, J. Corney, E. M. Wright, and D. F. Walls, Phys. Rev. A **55**, 4318 (1997).
[15] D. Ananikian and T. Bergeman, Phys. Rev. A **73**, 013604 (2006).
[16] G. S. Paraoanu, S. Kohler, F. Sols, and A. Leggett, J. Phys. B: At., Mol. Opt. Phys. **34**, 4689 (2001).
[17] A. Smerzi, S. Fantoni, S. Giovanazzi, and S. R. Shenoy, Phys. Rev. Lett. **79**, 4950 (1997).
[18] P. A. Braun, Rev. Mod. Phys. **65**, 115 (1993).
[19] Note that in Braun [18] ϕ is introduced as a momentum operator.
[20] Strictly speaking, the argument of the square root should read $(N+1)^2/4 - j^2$, which in the semiclassical limit may well be replaced by our expression.
[21] S. Raghavan, A. Smerzi, S. Fantoni, and S. R. Shenoy, Phys. Rev. A **59**, 620 (1999).
[22] M. Holthaus and S. Stenholm, Eur. Phys. J. B **20**, 451 (2001).
[23] G. J. Krahn and D. H. J. O'Dell, J. Phys. B **42**, 205501 (2009).

[24] J. Javanainen, Phys. Rev. A **81**, 051602(R) (2010).
[25] A. P. Tonel, J. Links, and A. Foerster, J. Phys. A: Math. Gen. **38**, 6879 (2005).
[26] T. Zibold, E. Nicklas, C. Gross, and M. K. Oberthaler, Phys. Rev. Lett. **105**, 204101 (2010).
[27] W. T. Strunz, G. Alber, and J. S. Briggs, J. Phys. B: At., Mol. Opt. Phys. **24**, 5091 (1991).
[28] R. Schinke, *Photodissociation Dynamics: Spectroscopy and Fragmentation of Small Polyatomic Molecules* (Cambridge University Press, Cambridge, 1995).
[29] L. Pitaevskii and S. Stringari, *Bose-Einstein Condensation* (Oxford University Press, Oxford, 2003).
[30] R. Paredes and E. Neri, J. Phys. B: At., Mol. Opt. Phys. **42**, 035301 (2009).